Oxygen-Transfer Reactions of Molybdenum- and Tungstendioxo Complexes Containing η^2-Pyrazolate Ligands

Kerstin Most, Jens Hoßbach, Denis Vidović, Jörg Magull, Nadia C. Mösch-Zanetti*

Institut für Anorganische Chemie, Georg-August-Universität Göttingen, Tammannstraße 4, 37077 Göttingen, Germany
Fax: (+49)-551-39-3373; e-mail: nmoesch@gwdg.de

Received: August 9, 2004; Accepted: November 22, 2004

Dedicated to Richard R. Schrock on the occasion of his 60th birthday

Supporting Information for this article is available on the WWW under http://asc.wiley-vch.de/home/.

Abstract: Dioxomolybdenum and -tungsten compounds containing sterically demanding pyrazolate ligands have been synthesised by treatment of dioxometal halides with the potassium salts of 3,5-di-*tert*-butylpyrazole (*t*-Bu$_2$pzH) and 3,5-di-*tert*-butyl-4-bromopyrazole (*t*-Bu$_2$-4-BrpzH). The products [MoO$_2$Cl(η^2-*t*-Bu$_2$pz)] (**1**), [MoO$_2$(η^2-*t*-Bu$_2$pz)$_2$] (**2**), [MoO$_2$(η^2-*t*-Bu$_2$-4-Brpz)$_2$] (**3**), [WO$_2$(η^2-*t*-Bu$_2$pz)$_2$] (**4**) and [WO$_2$(η^2-*t*-Bu$_2$-4-Brpz)$_2$] (**5**) were characterised by spectroscopic techniques. The X-ray structure of complex **3** reveals a distorted trigonal prismatic geometry with two η^2-co-ordinated pyrazolate ligands. These high-valent compounds participate in oxygen-transfer reactions and catalyse the oxidation of PPh$_3$ with dimethyl sulphoxide. UV/VIS measurements of the oxo-transfer reactions and the kinetics of the catalytic process are described. By the reaction of **2** with three equivalents of PEt$_3$ or treatment of [MoOCl$_2$(PMe$_3$)$_2$] with two equivalents of *t*-Bu$_2$pzK mononuclear mono-oxo compounds of the type [MoO(*t*-Bu$_2$pz)$_2$(PR$_3$)$_2$] (R = Et **6**, R = Me **7**) were obtained and characterised by X-ray diffraction analyses. This points to biologically relevant mononuclear Mo(IV) intermediates in the catalytic process with this type of complex.

Keywords: homogeneous catalysis; molybdenum; N,N ligands; oxo-transfer reactions; pyrazolates; tungsten

Introduction

Molybdenum- and tungsten-catalysed oxygen-transfer reactions have attracted considerable interest in recent years due to their relevance in biological processes.[1–3] Molybdenum is found in a class of enzymes that are commonly referred to as mononuclear molybdoenzymes or oxotransferases, that catalyse oxygen atom transfer to and from a substrate. Mononuclear tungsten enzymes are also known[4] but, in contrast to the well developed molybdenum chemistry, tungsten-mediated atom transfer reactions have been significantly less studied.[5–8] In recent years, crystal structures of several molybdo- and tungstoenzymes were determined.[9–13] In all cases, the reaction centre contains a mononuclear metal centre co-ordinated by one or two oxygen as well as one or two pterin ligands, whose dithiolene functionality co-ordinates to the metal atom. Model chemistry has been focussed on the use of MO_2^{2+} cores and on variation of the co-ligands LL′ ([LL′M^{VI}O$_2$], M = Mo, W) to influence the steric as well as the redox properties of the oxygen-transfer reaction. Pioneering research designing sulphur-based ligand systems for molybdenum-catalysed oxo-transfer reactions came from Holm and co-workers.[14–16] Thereafter, many N,O-, N,S- and S,S-based ligands systems were investigated.[17,18] Significantly less studied were anionic N,N-donors in spite of the fact that amido ligands have had a great impact on early transition metal chemistry.[19–22] Besides the thoroughly investigated tris(pyrazolyl)borate N-donor ligands by Enemark and co-workers,[23,24] producing a variety of interesting Mo(IV), Mo(V) and Mo(VI) complexes, only a few other N,N-donor ligand systems were studied.[25,26]

Pyrazolate ligands in general have been widely used to synthesise a variety of transition metal complexes.[27–30] The bridging co-ordination mode μ-η^1:η^1 of the pyrazolate anion between two metal atoms is prevalent, leading mainly to dimeric or oligomeric structures. By introducing sterically demanding groups in the 3- and 5-positions, mononuclear complexes of early transition metals were accessible that feature the unusual η^2-bonding mode.[31–35] Until recently, η^2-co-ordination was limited to d-block metals with empty d-shells. We[36,37] and oth-

 DOI: 10.1002/adsc.200404265

ers[38,39] have now demonstrated that reduced species are accessible and that η^2-co-ordination is retained.

The lack of nitrogen-based systems as well as our general interest in pyrazolate chemistry prompted us to investigate the use of such ligands to stabilise MO_2^{2+} cores (M = Mo, W) and the reactivity of such compounds in oxygen-transfer reactions. We recently communicated the syntheses and catalytic activity of molybdenum compounds containing η^2-*t*-Bu_2pz ligands.[40] We report here a more detailed investigation of such complexes and their oxygen-transfer properties, which includes analogous tungsten(VI) complexes as well as the syntheses and crystallographic characterisation of a mononuclear mono-oxomolybdenum(IV) complex.

Results

Synthesis of the Ligands and Complexes

The sterically demanding pyrazole ligand containing *tert*-butyl groups in the 3- and 5-positions (*t*-Bu_2pzH) and its potassium salt (*t*-Bu_2pzK) were prepared according to literature procedures.[41,42] The analogous pyrazole substituted by a bromine in the 4-position, 3,5-di-*tert*-butyl-4-bromopyrazole (*t*-Bu_2-4-BrpzH), was prepared according to an analogous procedure previously reported for 3,5-dimethyl-4-bromopyrazole.[43] Reaction of *t*-Bu_2pzH with one equivalent of $AgNO_3$ in ethanol led to an ill-defined silver salt of the ligand, which was not further characterised. Treatment of this salt with bromine in chloroform gave *t*-Bu_2-4-BrpzH in high yields [Eq.(1)].

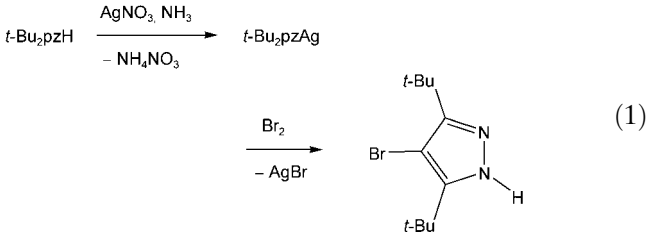

(1)

3,5-Di-*tert*-butyl-4-bromopyrazole was isolated as a slightly yellow solid, which is soluble in common organic solvents such as toluene, tetrahydrofuran and pentane. The ^{1}H NMR spectrum shows one resonance for protons of the *tert*-butyl groups (δ = 1.34 ppm) and one broad resonance for the N–H proton (δ = 10.3 ppm).

Syntheses of Molybdenum(VI) and Tungsten(VI) Complexes

Dioxomolybdenum(VI) and dioxotungsten(VI) compounds were obtained by reacting the appropriate metal chloride starting material with potassium salts of the ligands as shown in Scheme 1. Reaction of $[MoO_2Cl_2]$ with one or two equivalents of potassium 3,5-di-*tert*-butylpyrazolate (*t*-Bu_2pzK) in toluene at room temperature afforded $[MoO_2Cl(\eta^2$-*t*-Bu_2pz)] (**1**) and $[MoO_2(\eta^2$-*t*-Bu_2pz$)_2]$ (**2**) in good yields. Treatment of $[MoO_2Cl_2]$ with two equivalents of potassium 3,5-di-*tert*-butyl-4-bromopyrazolate (*t*-Bu_2-4-BrpzK) in toluene led to $[MoO_2(\eta^2$-*t*-Bu_2-4-Brpz$)_2]$ (**3**). The tungsten complexes $[WO_2(\eta^2$-*t*-Bu_2pz$)_2]$ (**4**) and $[WO_2(\eta^2$-*t*-Bu_2-4-Brpz$)_2]$ (**5**) were synthesised using the dimethoxyethane adduct $[WO_2Cl_2$(dme)], a more soluble starting material than the polymeric $[WO_2Cl_2]$.

Compounds **1** and **2** were purified by sublimation at 120–130 °C under reduced pressure to give pale yellow **1** and colourless **2**, pointing to a thermal stability of these complexes, whereas **3**–**5** were purified by recrystallisation from concentrated toluene solutions. Attempts at sublimation led to decomposition. The crystalline complexes **1**–**5** are readily soluble in common organic solvents such as toluene, tetrahydrofuran and pentane. They are stable in dry air, whereas moisture leads to immediate decomposition forming blue intractable solids.

The ^{1}H NMR spectra of compounds **1**–**5** in toluene-d_8 between +20 and −80 °C show for all five complexes one set of resonances each for symmetrically co-ordinated ligands (δ = 1.12, 6.09 ppm for **1**; 1.20, 6.29 ppm for **2**; 1.30 ppm for **3**; 1.18, 6.44 ppm for **4**; and 1.28 ppm for **5**). The ^{13}C NMR spectra of the complexes show the signal for the α-*C*, β-*C*, *C*$(CH_3)_3$ and C(*C*$H_3)_3$ (δ = 30.05, 32.09, 112.46, 160.94 ppm for **1**; 30.20, 32.37, 107.08, 162.30 ppm for **2**; 28.35, 33.47, 98.51, 157.47 ppm for **3**; and 30.05, 32.44, 108.57, 162.15 ppm for **4**). On mass spectrometry, the $[M^+]$ species with correct isotope pattern are observed. The IR spectra display two strong $\nu_{M=O}$ bands at 971 and 941 cm^{-1} for **1**, 951 and 922 cm^{-1}

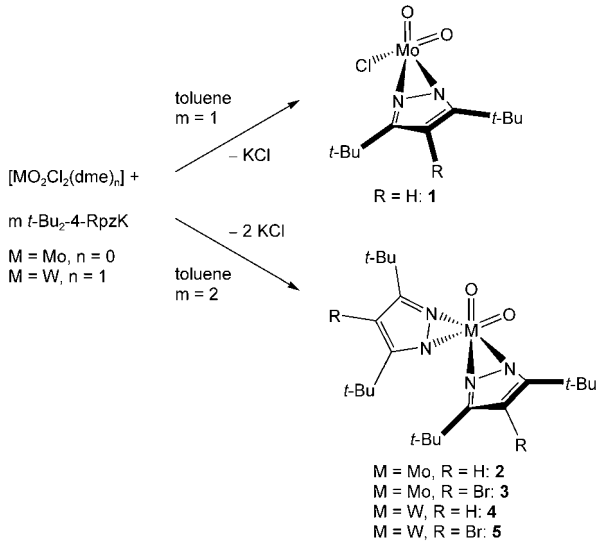

Scheme 1.

for **2**, 985 and 951 cm^{-1} for **3**, and 996 and 960 cm^{-1} for **4**, characteristic for the symmetric and asymmetric vibrational modes, respectively, of the *cis*-$[MO_2]^{2+}$ (M = Mo, W) fragment. All compounds are monomeric in solution as confirmed by molecular mass determination by vapour pressure osmometry in toluene. Solid state structures of compounds **2** and **4** were determined by X-ray single crystal analyses (*vide infra*).

Syntheses of Molybdenum(IV) Complexes

By reacting three equivalents of PEt_3 with **1** at 0 °C in pentane solution an immediate colour change to brown was observed. After evaporation of the solvent to a minimum amount and storage at −20 °C few green crystals appeared in the solution along with an unidentified brown precipitate. Single crystal X-ray analysis (*vide infra*) proved the green crystals to be the monomeric molybdenum(IV) mono-oxo compound $[MoO(t\text{-}Bu_2pz)_2(PEt_3)_2]$ (**6**) (Scheme 2). The occurrence of a monomeric Mo(IV)=O species rather than a μ-oxo-bridged $Mo(V)_2O_3$ species is of significant interest for the current study as discussed below. In addition, only few monomeric Mo(IV)=O compounds have been crystallographically characterised and even fewer η^2-pyrazolate complexes of reduced metal centres are known. Although several attempts were made by varying the reaction conditions as well as the solvent, the yield could not be increased, which is mainly due to the compound's sensitivity towards oxygen and moisture but also due to its high solubility in most organic solvents. Better yields were obtained by the direct reaction of $[MoOCl_2(PMe_3)_3]$ with two equivalents of $t\text{-}Bu_2pzK$ leading to the analogous complex $[MoO(t\text{-}Bu_2pz)_2(PMe_3)_2]$ (**7**) with co-ordinated PMe_3 rather than PEt_3 (Schema 2).

Both complexes are diamagnetic green solids that are readily soluble in common organic solvents. Spin-pairing in mono-oxomolybdenum(IV) compounds is a common feature, as the Mo−O bond dominates the ligand field.[44] In contrast to compounds **1**–**5**, the ^1H NMR spectra of **6** and **7** show resonances for two different *t*-Bu groups (δ = 1.40 and 1.60 ppm for **6**, 1.49 and 1.60 ppm for **7**) and one for the pyrazolate ring proton (δ = 6.05 ppm for **6** and 6.00 ppm for **7**) consistent with the solid state structure. The ^{31}P NMR spectrum of **7** shows one resonance at δ = 0.95 ppm. Compound **7** has also been characterized by electron impact (EI) mass spectrometry and the $[M^+ - PMe_3]$ species at m/z = 548 with correct isotopic distribution pattern has been identified. An attempted X-ray diffraction analysis of compound **7** confirms the connectivity and suggests an isostructural relationship to **6** but the dataset does not allow a discussion of bond lengths and angles. Complex **7** reacts with excess DMSO to give the dioxo compound **2** which was confirmed spectroscopically. The ^1H NMR spectrum of a sample of **7** in benzene-d_6 treated with excess DMSO-d_6 shows the resonances for **2** and $OPMe_3$ and the only resonance found in the ^{31}P NMR spectrum is that for $OPMe_3$. Electron impact mass spectrometry confirms the formation of **2**.

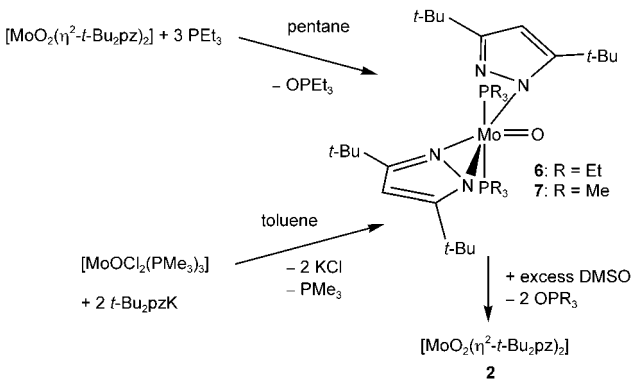

Scheme 2.

Molecular Structures of 3 and 6

Figure 1 shows the molecular structure of compound **3**. For selected bond lengths and angles as well as for the crystallographic data and structure refinement see Tables 1 and 2 in the Supporting Information.

Compound **3** crystallises in the orthorhombic space group $Pna2_1$ with one molecule in the asymmetric unit. The molybdenum atom is surrounded by two oxygen and four nitrogen atoms. The geometry is best described as a distorted trigonal prism rather than as an octahedron, since the largest angles between the oxygen atoms and any other co-ordinating atom are O(1)−Mo(1)−N(2) = 140.07(14)° and O(2)−Mo(1)−N(3) = 140.35(15)°. Both pyrazolate ligands with bond lengths differences of 0.164 Å for the N(1),N(2)-ligand

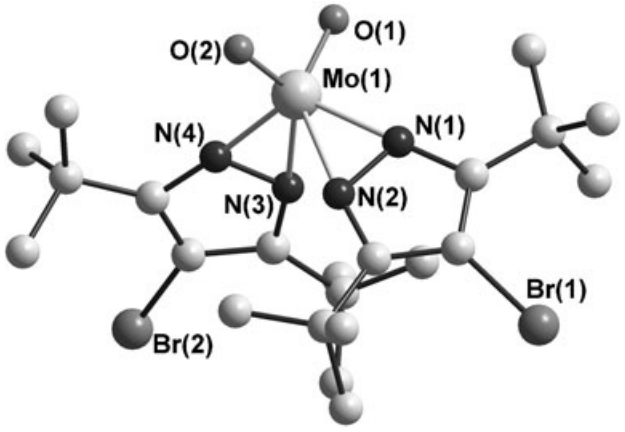

Figure 1. Molecular structure of $[MoO_2(\eta^2\text{-}t\text{-}Bu_2\text{-}4\text{-}Brpz)_2]$ (**3**).

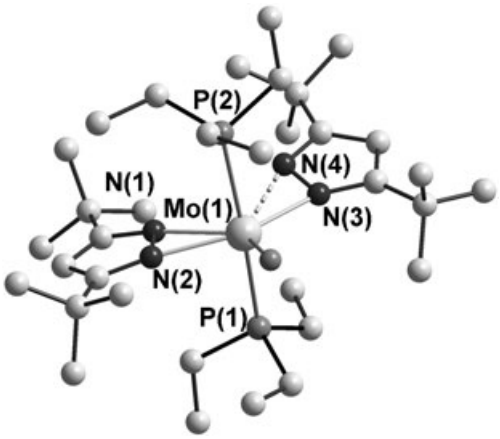

Figure 2. Molecular structure of [MoO(η^2-*t*-Bu_2pz)(η^1-*t*-Bu_2pz)(PEt_3)$_2$] (**6**).

and 0.174 Å for the N(3),N(4)-ligand can be described as 'slipped' η^2-co-ordinated, a denotation previously applied for this kind of asymmetric bonding.[32] The Mo=O bond lengths of 1.686(3) and 1.685(3) Å are in the same range to those found in **1**.[40] The dihedral angles between the N–Mo–N plane and N–C–C–C–N best plane are 17.7° for the N(1),N(2)-ligand and 9.9° for the N(3),N(4)-ligand.

The solid state structure of complex **6** is shown in Figure 2. Complex **6** crystallises in the monoclinic space group $P2_1/c$ with two independent molecules in the asymmetric unit. The two molecules have identical structural parameters within the standard deviation (see the table of selected bond lengths in the Supporting Information), so that only molecule 1 will be discussed.

The molybdenum atom is surrounded by four nitrogen and two phosphorus atoms as well as one oxygen atom. If the centre of the nitrogen-nitrogen bond in the N(1),N(2)-pyrazolate ligand is considered as a monodentate donor, the geometry about the molybdenum atom is best described as trigonal bipyramidal with the two phosphorus atoms being in the apical positions [P(1)–Mo(1)–P(2) = 172.09(3)°]. Similar to **3**, the N(1),N(2)-ligand with a bond length difference of 0.154 Å [Mo(1)–N(1) = 2.337(3), Mo(1)–N(2) = 2.183(3) Å] can be described as 'slipped' η^2-co-ordinate. In contrast, the N(3),N(4)-ligand is η^1-co-ordinate, since the Mo(1)–N(4) distance of 2.594 Å is too long to assume a bond. The Mo=O distance of Mo1–O1 = 1.656(2) Å is in the normal range for this type of complex.[44,45] The trigonal bipyramidal geometry contrasts with that of [$MoOCl_2(PMe_3)_3$][45] as well as that of [$MoO(acac)_2(PMe_3)$][46] where distorted octahedral geometries are observed. Only few mononuclear Mo(IV)=O compounds with co-ordinated phosphine ligands have been structurally characterised.[46–49] The two pz ligands in **6** are approximately coplanar with each other as well as with the metal atom. This structural feature is found in several η^2-co-ordinate azolate complexes,[31,36,50] suggesting the possibility of π-donor interactions between the two ligands and *d*-orbitals of the metal.

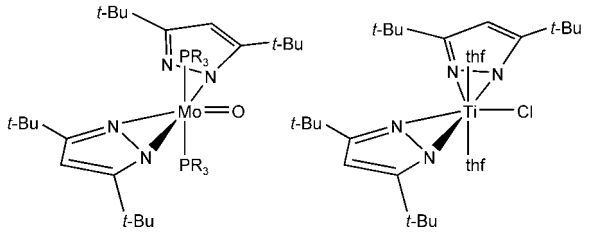

In particular, the titanium(III) compound [Ti(η^2-*t*-Bu_2pz)$_2$Cl(thf)$_2$] displays a very similar overall structure with the two pz ligands and the titanium atom in one plane and the two tetrahydrofuran molecules co-ordinated to Ti above and below this plane.[36] However, in the d^1 system both pz ligands co-ordinate η^2, although the metal-nitrogen bonds are in a similar range arguing against steric factors for the opening of one metal-ligand bond in compound **6**. Theoretical calculations on the titanium and molybdenum compounds confirming these electronic features are currently being investigated.

Molecular Structure of *t*-Bu_2-4-BrpzH

The molecular structures of the complexes were complemented by determination of the structure of the bromine-substituted ligand *t*-Bu_2-4-BrpzH. Comparison to that of previously characterised *t*-Bu_2pzH shows the bromine atom exerting little structural influence.[51,52] However, whereas the *tert*-butyl groups of *t*-Bu_2pzH are rotationally disordered, the additional bromine atom in *t*-Bu_2-4-BrpzH seems to prevent it as no disorder is observed. The molecular structure is shown in Figure 3 along with selected bond lengths and angles.

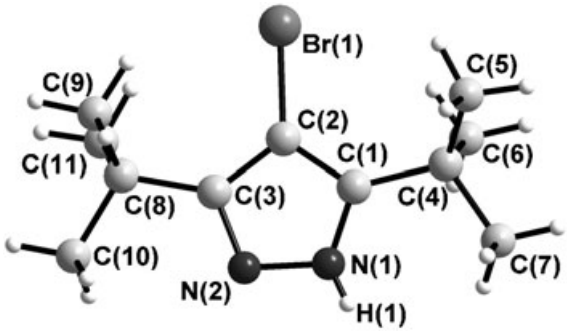

Figure 3. Molecular structure of *t*-Bu_2-4-BrpzH. Selected bond lengths [Å] and angles [°]: Br(1)–C(2) 1.877(6), Br(2)–C(13) 1.901(6), N(1)–C(1) 1.338(8), N(3)–C(12) 1.362(8), C(1)–C(2) 1.392(8), C(2)–C(3) 1.410(8), N(2)–C(3) 1.353(8), N(1)–N(2) 1.357(7), N(3)–N(4) 1.354(7), C(1)–N(1)–N(2) 110.4(5), C(1)–C(2)–C(3) 107.0(5).

Oxo-Transfer Reactions

The reaction of $[MoO_2(t\text{-}Bu_2pz)_2]$ (**2**) with one equivalent of triphenylphosphine in toluene-d_8 at 80 °C was monitored by ^{31}P NMR spectroscopy.[40] Over the course of 3 hours, the reaction solution turned gradually brown and remained clear throughout the reaction time. The only two resonances observed were those for PPh_3 and $OPPh_3$. The phosphine was oxidised by the molybdenum compound, but the reaction did not proceed after 80% conversion. In addition, oxo-transfer from **2** to triphenylphosphine was monitored by UV/VIS spectrophotometry as shown in Figure 4. In the UV/VIS reactions the ratio between Mo:PPh_3 was 1:50. All reaction solutions turned gradually brown and remained clear throughout the reaction time. The maximum at 450 nm increases for the 2.6 hours as the reaction proceeds (Figure 5). Thereafter, the maximum at 450 decreases and the one at 753 nm increases (Figure 6). For the first process, a clean isosbestic point is found at 345 nm whereas for the second process isosbestic points at 334, 422 and 640 nm are found. The chosen ratio between Mo:PPh_3 of 1:50 would allow a first order treatment of the reaction. However, the overlay of the two processes prevented the analysis of the kinetics.

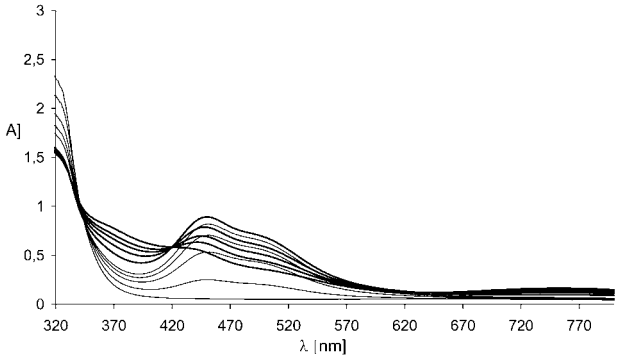

Figure 4. Reduction of **2** in toluene at 80 °C. Thin and thick lines indicate two processes at different times (thin lines first process, thick lines second process).

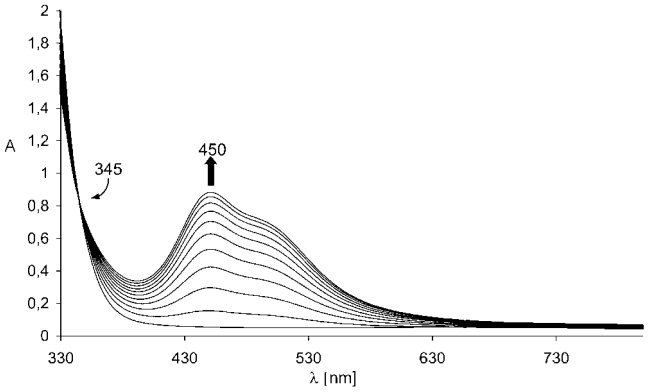

Figure 5. Reduction of **2** in toluene at 80 °C. Spectra recorded from $t = 0$ to 160 minutes.

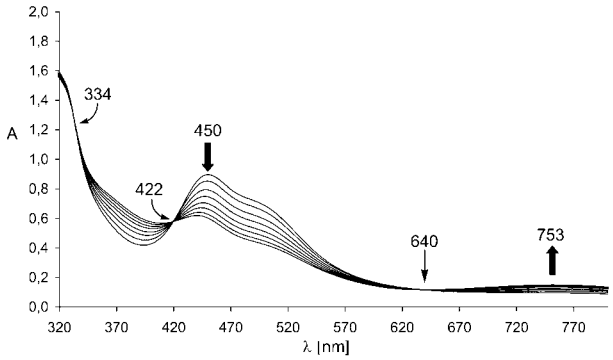

Figure 6. Reduction of **2** in toluene at 80 °C. Spectra recorded from $t = 260$ to 950 minutes.

Catalysis of the Oxo-Transfer

The reduction of complex **2** by oxo-transfer can be coupled to its reoxidation by the reaction with dimethyl sulphoxide leading to catalytic transfers. Ten equivalents of $P(p\text{-}C_6H_4F)_3$ in DMSO in the presence of **2** are completely converted to $OP(p\text{-}C_6H_4F)_3$. Reaction solutions remain colourless during the entire catalysis. The progress of the reaction was monitored by ^{19}F NMR spectroscopy at four different temperatures. NMR spectra show the decrease of the resonance for the fluorine in $P(p\text{-}C_6H_4F)_3$ and the increase of that in $OP(p\text{-}C_6H_4F)_3$ (Figure 7). No other resonances were detected. DMSO and $P(p\text{-}C_6H_4F)_3$ do not react under these conditions without catalyst.

Because DMSO was in excess over $P(p\text{-}C_6H_4F)_3$ and **2**, the reaction should be first-order in the concentration of the phosphine. Phosphine oxidation is the rate-limiting step, so that reoxidation of the molybdenum complex is probably fast and its concentration may be assumed constant. The rate law shown in Eq. (2) or (3) is therefore applicable and plots of $\ln(\{c[P(p\text{-}C_6H_4F)_3] + c[OP(p\text{-}C_6H_4F)_3]\}/c\{c[P(p\text{-}C_6H_4F)_3]$ *vs.* t should give linear relationships whose slopes are consistent with k divided by the concentration of the metal complex.

$$c[P(C_6H_4F)_3] = c_0[P(C_6H_4F)_3] \cdot e^{-k \cdot c([MoO_2(t\text{-}Bu_2pz)_2]) \cdot t} \quad (2)$$

$$\ln\left(\frac{c[P(C_6H_4F)_3] + c[OP(C_6H_4F)_3]}{c[P(C_6H_4F)_3]}\right) = k \cdot c([MoO_2(t-Bu_2pz)_2]) \cdot t \quad (3)$$

The catalytic reactions with compound **2** gave linear relationships over the entire period. Values for $k \cdot c([MoO_2(t\text{-}Bu_2pz)_2]) = k_{cat}$ determined are given in Table 1.

The Eyring plot ($\ln(h \cdot k_{cat}/k_B \cdot T) \cdot R$ *vs.* $-1/T$ (h = Planck's constant, k_B = Boltzmann constant, R gas con-

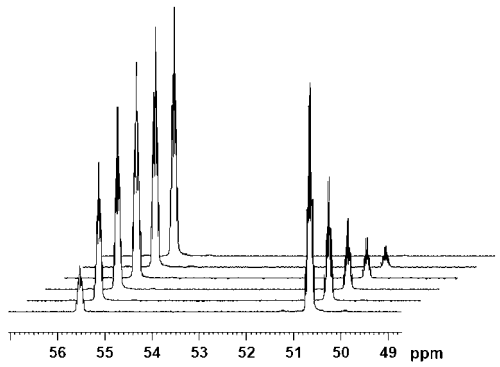

Figure 7. ^{19}F NMR spectra recorded at $T = 333$ K in toluene initially containing $3.9 \cdot 10^{-4}$ mol/L $P(p\text{-}C_6H_4F)_3$ and $3.9 \cdot 10^{-5}$ mol/L $[MoO_2(t\text{-}Bu_2pz)_2]$, every 15 minutes.

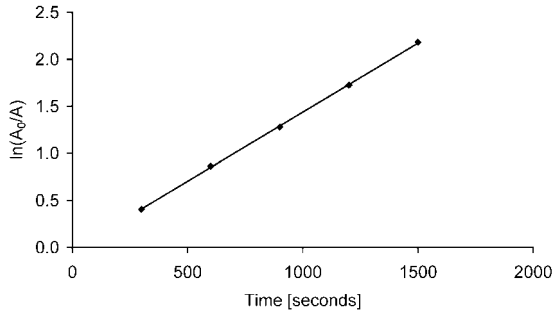

Figure 8. Typical plot of $\ln(A_0/A)$ *vs.* time, shown for $T = 353$ K $\{A_0 = c[P(p\text{-}C_6H_4F)_3] + c[OP(p\text{-}C_6H_4F)_3]$, $A = c[P(p\text{-}C_6H_4F)_3]\}$.

stant) gives a linear relationship and its slope and axis intercept lead to activation enthalpy and entropy of $\Delta H^{\#} = 77.7$ kJ/mol and $\Delta S^{\#} = -81$ J/K·mol.

The analogous reaction of the tungsten compound $[WO_2(t\text{-}Bu_2pz)_2]$ with $P(p\text{-}C_6H_4F)_3$ in DMSO at 80 °C led also to the oxidation of the phosphine, although significantly slower than its molybdenum analogue. In typical experiments containing $c\{[WO_2(t\text{-}Bu_2pz)_2]\} = 3.9 \cdot 10^{-4}$ M and $c[P(C_6H_4F)_3] = 3.9 \cdot 10^{-3}$ M values for k_{cat} and k are $1.92 \cdot 10^{-4}\ s^{-1}$ and $4.92\ M^{-1}\ s^{-1}$, respectively. In the absence of DMSO, no oxo-transfer reaction occurred from $[WO_2(t\text{-}Bu_2pz)_2]$ to $P(C_6H_4F)_3$ at up to 80 °C.

Table 1. Rate constants k_{cat} and k for the oxidation of $P(p\text{-}C_6H_4F)_3$ with DMSO catalysed by $[MoO_2(t\text{-}Bu_2pz)_2]$ at different temperatures.

T [K]	k_{cat} [s^{-1}]	k [$s^{-1} \cdot M^{-1}$]
223	$1.09 \cdot 10^{-4}$	4.87
233	$3.05 \cdot 10^{-4}$	7.82
243	$6.40 \cdot 10^{-4}$	16.41
253	$1.44 \cdot 10^{-3}$	36.92

Discussion

Structural Aspects

Several crystal structures of DMSO reductase from *Rhodobacter sphaeroides* or *Rhodobacter capsulatus* have revealed considerable variability in the structure of the active site, so that mechanistic aspects are still unclear.[10–12] In this regard, the position of the pterin-sulphur atoms is controversially discussed.[11,12,53] However, a recent high resolution X-ray structure of DMSO reductase (1.3 Å) suggests that the co-ordination geometry of the oxidised enzyme seems to be best described as distorted trigonal prismatic with four sulphur and two oxygen atoms co-ordinated to the metal.[11] This structural situation should be compared with that of compound $[MoO_2(t\text{-}Bu_2\text{-}4\text{-}Brpz)_2]$ (**3**). Although the co-ordinating atoms differ from those in the natural system, the co-ordination geometry of **3** is comparable. The distorted trigonal prism approaches the situation in the structure of DMSO reductase. In both geometries the oxo ligands are not *trans* to any sulphur or nitrogen ligand, respectively. This situation is different from most other model compounds for this type of enzyme as they usually provoke distorted octahedral geometries with ligands *trans* to the oxo groups.[54] In the pyrazolate complexes, the small bite angle of the ligand prevents an octahedral geometry. Therefore, the pyrazolate complex represents a rare example of a co-ordinational model for DMSO reductase.

Oxo-Transfer Reactivity

Oxo-transfer is accompanied by the formation of a μ-oxo dimer as shown in Scheme 3, unless it is prevented by sterically demanding ligands as is found in nature.

Dimerisations are found to be reversible and irreversible.[2] Reversible reactions performed with a molybdenum to phosphine ratio of 1:1 lead to complete oxidation of the phosphine, whereas irreversible reactions lead only to 50% conversion. Therefore, to answer the question whether a μ-oxo compound is formed as an intermediate, ultimately the isolation and structural characterisation of the reduced species is necessary.

We were able to isolate and structurally characterise the reduced compound $[MoO(t\text{-}Bu_2pz)_2(PEt_3)_2]$ (**6**) which proved to be mononuclear. This strongly suggests

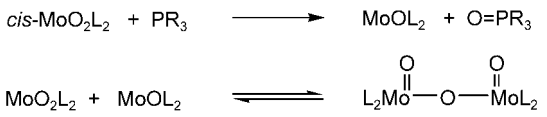

Scheme 3.

the occurrence of a mononuclear intermediate in oxo-transfer reactions of this system. However, kinetic studies employing low as well as high concentrations of phosphine *vs.* molybdenum point to two different pathways. In oxo-transfer reactions employing a 1:1 ratio of **2** and PR_3 80% conversion to OPR_3 is found which contrasts the theoretical 33% in the case where $[MoO(t\text{-}Bu_2pz)_2(PR_3)_2]$ represents the only species formed. We believe that the low phosphine concentration leads to competitive formation of the μ-oxo dimer, which is presumably unstable under the employed reaction conditions (80 °C). Therefore, several attempts to isolate a μ-oxo compound failed. At high concentrations of phosphine (excess PPh_3 *vs.* molybdenum), two stepwise processes are involved both showing clean isosbestic points in the UV/VIS spectra. Whereas in the first process a species is formed showing a maximum at 450 nm, it disappears in the second process. This points to the reduction of $[MoO_2(t\text{-}Bu_2pz)_2]$ to $[MoO(t\text{-}Bu_2pz)_2(PPh_3)_2]$ in the first process, but under the reaction conditions (excess phosphine) further reduction occurs to an as yet unknown molybdenum compound. For this reason, rate laws could not be determined. The kinetic investigation together with the isolation and crystallographic characterisation of $[MoO(t\text{-}Bu_2pz)_2(PEt_3)_2]$ suggest that oxo-transfer is possible in the here reported system forming initially a mononuclear molybdenum pyrazolate complex but two different decomposition pathways occur depending on the phosphine concentration.

Catalytic Oxo-Transfer Reactivity

In contrast to the oxo-transfer discussed above, catalytic oxo-transfer reactions are not hampered by decomposition reactions. Complex $[MoO_2(t\text{-}Bu_2pz)_2]$ cleanly catalyses the oxidation of trisubstituted phosphines. Oxo-transfer occurs from dimethyl sulphoxide to the phosphine forming dimethyl sulphide and the oxidised phosphine. By using excess DMSO, pseudo-first-order conditions are observed and kinetic measurements show linear relationships $\ln[c(PR_3)]$ *vs.* time throughout the reaction pointing to the catalyst's stability under these conditions. By varying the temperature, activation parameters were obtained ($\Delta H^{\#} = 77.7$ kJ/mol, $\Delta S^{\#} = -81$ J/K·mol). The large negative value for the entropy suggests an associative mechanism similar to previously described systems.[18,55,56] The rate-limiting step is presumably the oxidation of the phosphine indicated by the colour of the reaction solution which remained colourless. Fast oxidation of the reduced molybdenum species by DMSO reforming **2** has been experimentally established (Scheme 2). The catalytic cycle shown in Scheme 4 may be considered.

We believe that in the catalytic reaction a species of the type $[MoO(t\text{-}Bu_2pz)_2(L)_2]$ is formed. The first step represents the formation of an OPR_3 co-ordinated complex. The isolation of such an OPR_3 adduct has recently been reported in a trispyrazolylborate complex.[57] Under excess DMSO conditions the phosphine oxide is substituted forming a sulphoxide complex that cannot be isolated as it converts quickly to **2**.

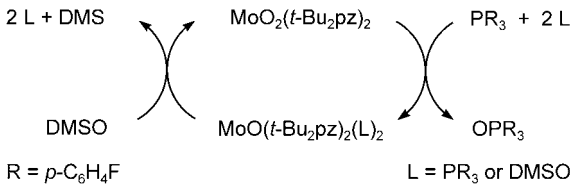

Scheme 4. Catalytic oxo-transfer showing the presumed intermediates.

In comparison to molybdenum, oxo-transfer reactions employing tungsten compounds are far less investigated.[5,7,17,58–60] Conversions are usually significantly slower or do not occur at all, which is certainly due to the higher redox potential found in the higher homologue. It is therefore of interests that the analogous tungsten compound $[WO_2(t\text{-}Bu_2pz)_2]$ catalyses the oxidation of $P(C_6H_4F)_3$ to $OP(C_6H_4F)_3$, albeit much slower than the Mo analogue. This represents a rare example of a nitrogen-based tungsten system that catalyses the oxidation of phosphines. The reactivity towards better oxygen acceptors that might allow the isolation of reduced tungsten compound is currently being investigated in our laboratory.

Conclusion

Sterically demanding pyrazolate ligands have been found to stabilise oxomolybdenum and oxotungsten compounds. The ligands co-ordinate either in the unusual η^2- or η^1-mode depending on the steric situation within the complex. The dioxo compounds are capable of oxidising phosphines by oxo-transfer reaction from dimethyl sulphoxide. The use of DMSO as oxo donor in this study has biological relevance to molybdenum-containing DMSO-reductases, which are able to utilise a variety of dialkyl and alkyl aryl sulphoxides as oxidizing substrates. Reduction of $[MoO_2(t\text{-}Bu_2pz)_2]$ by addition of PEt_3 leads to $[MoO(t\text{-}Bu_2pz)_2(PEt_3)_2]$ (**6**), which allows the conclusion that a monomeric Mo(IV)=O intermediate is involved in the catalytic cycle under appropriate conditions (co-ordinating solvents or excess phosphine).

Experimental Section

General Remarks

All manipulations were carried out under dry nitrogen using standard Schlenk-line or glove-box techniques. All solvents were purified by standard methods and distilled under a nitro-

gen atmosphere immediately prior to use. The starting materials $[MoO_2Cl_2]$,[61] $[WO_2Cl_2(dme)]$,[62] $[MoOCl_2(PMe_3)_3]$,[63] $P(C_6H_4F)_3$,[64] and *t*-Bu_2pzK[42] were prepared according to literature procedures. All other chemicals mentioned were used as purchased from commercial sources.

Samples for infrared spectroscopy were prepared as toluene solutions and measured on a BIO-RAD Digilab FTS-7, mass spectrometer were recorded with a Finnigan MAT 95 and all NMR spectra on a Bruker Avance 500 or 200. UV/VIS samples were prepared in a well-maintained grove-box with dry solvents and measured on the spectrophotometer analytikjena AG Specord S 100 equipped with a thermostat heating block. Elemental analyses were performed by the Analytisches-Chemisches Laboratorium des Instituts für Anorganische Chemie, Göttingen.

3,5-Di-*tert*-butyl-4-bromopyrazole (*t*-Bu_2-4-BrpzH)

In analogy to the procedure reported for the synthesis of silver 3,5-dimethylpyrazolate,[43] 3,5-di-*tert*-butylpyrazole (1.00 g, 1.0 equiv., 5.43 mmol) was suspended in ethanol (50 mL) and treated with 1 mL of NH_3 (conc.). Silver nitrate (0.922 g, 1.0 equiv., 5.43 mmol) was added to the solution and the reaction mixture was stirred for 12 h at ambient temperature. The solvent was removed under reduced pressure and the colourless residue was extracted with water. After filtration and evaporation of the solvent *t*-Bu_2-4-BrpzAg was obtained as colourless crystals; yield: 91%.

To a solution of *t*-Bu_2-4-BrpzAg (3.00 g, 1 equiv., 10.5 mmol) in CH_2Cl_2 (75 mL) bromine (1.84 g, 1.1 equiv., 11.5 mmol) was added and the reaction mixture was refluxed for 16 h. After filtration, the filtrate was washed with an aqueous solution of NaOH and the organic layer dried with $MgSO_4$. Evaporation of the solvent afforded *t*-Bu_2-4-BrpzH as yellow crystals; yield: 90%. ^{1}H NMR (C_6D_6): δ = 1.34 (s, 18H, *t*-Bu), 10.3 (br s, 1H, NH); ^{13}C NMR (C_6D_6): δ = 152.0 (s, 4C, α-*C*), 97.6 (s, 2C, β-*C*), 32.7 [s, 4C, *C*(CH_3)$_3$), 28.7 [s, 12C, C(*C*H_3)$_3$); MS: *m/z* = 258 (M^+), 243 (M^+ – Me); anal. calcd. for $C_{11}H_{19}N_2Br$: C 50.97, H 7.39, N, 10.81; found: C 49.7, H 7.2, N, 10.4.

Potassium 3,5-Di-*tert*-butyl-4-bromo-pyrazolate (*t*-Bu_2-4-BrpzK)

A solution of *t*-Bu_2-4-BrpzH (3 g, 11.6 mmol) in 30 mL of tetrahydrofuran was treated with excess KH (1.85 g, 46.3 mmol) and stirred at room temperature for 8 hours. Filtration through a pad of Celite and evaporation of the solvent gave the product as a colourless, microcrystalline material; yield: 2.45 g (71%). ^{1}H NMR (CD_3CN): δ = 1.33 (s, 18H, *t*-Bu).

General Procedure for the Preparation of the Molybdenum(VI) and Tungsten(VI) Compounds 1 – 5

A 100-mL Schlenk flask was charged with $[MO_2Cl_2(dme)_n]$ (M = Mo, n = 0; M = W, n = 1) and one or two equivalents of the appropriate potassium salt *t*-Bu_2-4-RpzK and toluene (30–50 mL). The reaction mixture was stirred for 15 h at ambient temperature and than filtered through a 2.5-cm pad of Celite. The solution was evaporated to dryness and the crude product was isolated. Recrystallisation from toluene gave the pure compounds in the 70 to 89% yields. See the Supporting Information for the characterisation data for compounds **1–5**.

[MoO(η^2-*t*-Bu_2pz)(η^1-*t*-Bu_2pz)(PEt_3)$_2$] (6)

To a solution of **2** (0.20 g, 0.41 mmol) in pentane, PEt_3 (0.15 g, 3 equivs., 1.23 mmol) was added slowly at 0 °C. The reaction mixture was stirred for 15 h at ambient temperature. After the volume of solvent was reduced under vacuum to approximately 5 mL, the solution was stored at −24 °C to obtain green crystals. ^{1}H NMR (C_6D_6): δ = 0. 98 (br s, 18H, CH_2CH_3), 1.43 (br s, 12H, CH_2CH_3). 1.40 (s, 18H, *t*-Bu*H*), 1.60 (s, 18H, *t*-Bu*H*), 6.05 (s, 2H, ring-*H*).

[MoO(η^2-*t*-Bu_2pz)(η^1-*t*-Bu_2pz)(PMe_3)$_2$] (7)

A solution of $[MoOCl_2(PMe_3)_3]$ (0.28 g, 0.68 mmol) in toluene (20 mL) was added to a suspension of *t*-Bu_2pzK (0.30 g, 2 equivs., 1.36 mmol) in toluene (10 mL) and stirred for 15 h. After filtration through a 2.5-cm pad of Celite, the volume of solvent was reduced to approximately 5 mL and the solution was stored at −24 °C to get green crystals of **7**; yield: 0.15 g (35%). ^{1}H NMR (C_6D_6): δ = 0.72 (s, 18H, Me*H*, 1.49 (s, 18H, *t*-Bu*H*), 1.60 (s, 18H, *t*-Bu*H*), 6.05 (s, 2H, ring-*H*); MS-EI: *m/z* = 548 (M^+ – PMe_3), 532 (M^+ – PMe_3 – O), 472 (M^+ – 2 PMe_3); anal. calcd. for $C_{28}H_{56}MoN_4OP_2$: C 53.55, H 8.83, N 9.30; found: C 54.01, H 9.07, N 9.00.

X-Ray Crystallography

Crystallographic data (excluding structure factors) for the structures reported in this paper have been deposited with the Cambridge Crystallographic Data Centre as supplementary publication nos. CCDC-246863 (**3**), CCDC-246862 (**6**) and CCDC-246864 (*t*-Bu_2-4-BrpzH). Copies of the data can be obtained free of charge on application to CCDC, 12 Union Road, Cambridge CB2 1EZ, UK [fax.: (internat.) +44 1223/336-033; e-mail: deposit@ccdc.cam.ac.uk].

See the Supporting Information for the X-ray crystallography of compounds **3** and **6** and selected crystallographic data.

Acknowledgements

This research was supported by a Grant from the Deutsche Forschungsgemeinschaft MO 963/2.

References

[1] R. H. Holm, *Coord. Chem. Rev.* **1990**, *100*, 183–221.
[2] J. H. Enemark, C. G. Young, *Adv. Inorg. Chem.* **1993**, *40*, 1–79.
[3] R. Hille, *Chem. Rev.* **1996**, *96*, 2757–2816.
[4] M. K. Johnson, D. C. Rees, W. W. Adams, *Chem. Rev.* **1996**, *96*, 2817–2839.
[5] G. C. Tucci, J. P. Donahue, R. H. Holm, *Inorg. Chem.* **1998**, *37*, 1602–1608.

[6] E. S. Davies, G. M. Aston, R. L. Beddoes, D. Collison, A. Dinsmore, A. Docrat, J. A. Joule, C. R. Wilson, C. D. Garner, *J. Soc. Chem., Dalton Trans.* **1998**, 3647–3656.
[7] K.-M. Sung, R. H. Holm, *Inorg. Chem.* **2001**, *40*, 4518–4525.
[8] Y.-L. Wong, Q. Yang, Z.-Y. Zhou, H. K. Lee, T. C. Mak, D. K. P. Ng, *New J. Chem.* **2001**, *25*, 353–357.
[9] M. K. Chan, S. Mukund, A. Kletzin, M. W. W. Adams, D. C. Rees, *Science* **1995**, *267*, 1463–1469.
[10] H. Schindelin, C. Kisker, J. Hilton, K. V. Rajagopalan, D. C. Rees, *Science* **1996**, *272*, 1615–1621.
[11] H.-K. Li, C. Temple, K. V. Rajagopalan, H. Schindelin, *J. Am. Chem. Soc.* **2000**, *122*, 7673–7680.
[12] R. C. Bray, B. Adams, A. T. Smith, B. Bennett, S. Bailey, *Biochemistry* **2000**, *39*, 11258–11269.
[13] H. Dobbek, R. Huber, *Met. Ions Biol. Syst.* **2002**, *39*, 227–263.
[14] J. M. Berg, R. H. Holm, *J. Am. Chem. Soc.* **1985**, *107*, 917–925.
[15] C. J. Doonan, D. A. Slizys, C. G. Young, *J. Am. Chem. Soc.* **1999**, *121*, 6430–6436.
[16] S. F. Gheller, B. E. Schultz, M. J. Scott, R. H. Holm, *J. Am. Chem. Soc.* **1992**, *114*, 6934–6935.
[17] J. H. Enemark, J. J. Cooney, J.-J. Wang, R. H. Holm, *Chem. Rev.* **2004**, *104*, 1175–1200.
[18] A. Thapper, C. Lorber, J. Fryxelius, A. Behrens, E. Nordlander, *J. Inorg. Biochem.* **2000**, *79*, 67–74.
[19] R. R. Schrock, *Pure Appl. Chem.* **1997**, *69*, 2197–2203.
[20] R. R. Schrock, *Acc. Chem. Res.* **1997**, *30*, 9–16.
[21] R. Kempe, *Angew. Chem.* **2000**, *112*, 478–504.
[22] L. H. Gade, *Chem. Commun.* **2000**, 173–181.
[23] Z. Xiao, C. G. Young, J. H. Enemark, A. G. Wedd, *J. Am. Chem. Soc.* **1992**, *114*, 9194–9195.
[24] Z. Xiao, M. A. Bruck, J. H. Enemark, C. G. Young, A. G. Wedd, *Inorg. Chem.* **1996**, *35*, 7508–7515.
[25] H. W. Roesky, B. Meller, M. Noltemeyer, H.-G. Schmidt, U. Scholz, G. M. Sheldrick, *Chem. Ber.* **1988**, *121*, 1403–1406.
[26] H. K. Lee, Y.-L. Wong, Z.-Y. Zhou, Z.-Y. Zhang, D. K. P. Ng, T. C. W. Mak, *J. Chem. Soc. Dalton Trans.* **2000**, 539–544.
[27] S. Trofimenko, *Prog. Inorg. Chem.* **1986**, *34*, 115–210.
[28] A. P. Sadimenko, S. S. Basson, *Coord. Chem. Rev.* **1996**, *147*, 247–297.
[29] G. La Monica, G. A. Ardizzoia, *Prog. Inorg. Chem.* **1997**, *46*, 151–238.
[30] A. P. Sadimenko, *Adv. Heterocycl. Chem.* **2001**, *80*, 157–240.
[31] I. A. Guzei, A. G. Baboul, G. P. A. Yap, A. L. Rheingold, H. B. Schlegel, C. H. Winter, *J. Am. Chem. Soc.* **1997**, *119*, 3387–3388.
[32] I. A. Guzei, G. P. A. Yap, C. H. Winter, *Inorg. Chem.* **1997**, *36*, 1738–1739.
[33] I. A. Guzei, C. H. Winter, *Inorg. Chem.* **1997**, *36*, 4415–4420.
[34] C. Yélamos, M. J. Heeg, C. H. Winter, *Inorg. Chem.* **1999**, *38*, 1871–1878.
[35] C. Yélamos, M. J. Heeg, C. H. Winter, *Organometallics* **1999**, *18*, 1168–1176.
[36] N. C. Mösch-Zanetti, R. Krätzner, C. Lehmann, T. R. Schneider, I. Usón, *Eur. J. Inorg. Chem.* **2000**, 13–16.
[37] K. Most, N. C. Mösch-Zanetti, D. Vidovic, J. Magull, *Organometallics* **2003**, *22*, 5485–5490.
[38] K. R. Gust, J. E. Knox, M. J. Heeg, H. B. Schlegel, C. H. Winter, *Eur. J. Inorg. Chem.* **2002**, 2327–2334.
[39] K. R. Gust, J. E. Knox, M. J. Heeg, H. B. Schlegel, C. H. Winter, *Angew. Chem.* **2002**, *114*, 1661–1664.
[40] K. Most, S. Köpke, F. Dall'Antonia, N. C. Mösch-Zanetti, *Chem. Commun.* **2002**, 1676–1677.
[41] C. Fernandéz-Castano, C. Foces-Foces, N. Jagerovic, J. Elguero, *J. Mol. Struct.* **1995**, *355*, 265–271.
[42] C. Yélamos, M. J. Heeg, C. H. Winter, *Inorg. Chem.* **1998**, *37*, 3892–3894.
[43] H. Reimlinger, A. Noels, J. Jadot, A. v. Overstraeten, *Chem. Ber.* **1970**, *103*, 1942–1948.
[44] C. D. Garner, J. M. Charnock, in: *Comprehensive Coordination Chemistry*, Vol. 3, (Eds.: G. Wilkinson, R. D. Gillard, J. A. McCleverty), Pergamon, Oxford, **1987**, pp. 1329–1374.
[45] K. Yoon, G. Parkin, A. L. Rheingold, *J. Am. Chem. Soc.* **1992**, *114*, 2210–2218.
[46] R. D. Roger, E. Carmona, A. Galindo, J. L. Atwood, L. G. Canada, *J. Organomet. Chem.* **1984**, *277*, 403–415.
[47] K. M. Nicholas, M. A. Khan, *Inorg. Chem.* **1987**, *26*, 1633–1636.
[48] B. Antelmann, G. Huttner, U. Winterhalter, *J. Organomet. Chem.* **1998**, *555*, 119–125.
[49] H. Liu, M. J. Calhorda, V. Felix, M. G. B. Drew, *J. Organomet. Chem.* **2001**, *632*, 175–187.
[50] N. C. Mösch-Zanetti, M. Hewitt, T. R. Schneider, J. Magull, *Eur. J. Inorg. Chem.* **2002**, 1181–1185.
[51] F. Aguilar-Parrila, H.-H. Limbach, C. Foces-Foces, F. H. Cano, N. Jagerovic, J. Elguero, *J. Org. Chem.* **1995**, *60*, 1965–1970.
[52] G. B. Deacon, A. Gitlits, P. W. Roesky, M. R. Bürgstein, K. C. Lim, B. W. Skelton, A. H. White, *Chem. Eur. J.* **2001**, *7*, 127–138.
[53] S. D. Garton, J. Hilton, H. Oku, B. R. Crouse, K. V. Rajagopalan, M. K. Johnson, *J. Am. Chem. Soc.* **1997**, *119*, 12906–12916.
[54] C. G. Young, in: *Comprehensive Coordination Chemistry II*, Vol. 4, (Eds.: J. A. McCleverty, T. J. Meyer), Elsevier, Oxford, **2004**, p. 416.
[55] B. E. Schultz, R. H. Holm, *Inorg. Chem.* **1992**, *32*, 4244–4248.
[56] C. Lorber, M. R. Plutino, L. I. Elding, E. Nordlander, *J. Chem. Soc. Dalton Trans.* **1997**, 3997–4003.
[57] P. D. Smith, A. J. Millar, C. G. Young, A. Ghosh, P. Basu, *J. Am. Chem. Soc.* **2000**, *122*, 9298–9299.
[58] S. Lee, D. L. Staley, A. L. Rheingold, N. J. Cooper, *Inorg. Chem.* **1990**, *29*, 4391–4396.
[59] A. A. Eagle, E. R. T. Tiekink, C. G. Young, *Inorg. Chem.* **1997**, *36*, 6315–6322.
[60] K.-M. Sung, R. H. Holm, *J. Am. Chem. Soc.* **2002**, *124*, 4312–4320.
[61] V. C. Gibson, T. P. Kee, A. Shaw, *Polyhedron* **1990**, *9*, 2293–2298.

[62] K. Dreisch, C. Andersson, C. Stalhandske, *Polyhedron* **1991**, *10*, 2417–2421.
[63] C. Limberg, M. Büchner, K. Heinze, O. Walter, *Inorg. Chem.* **1997**, *36*, 872–879.
[64] A. W. Johnson, H. L. Jones, *J. Am. Chem. Soc.* **1968**, *90*, 5232–5236.

